Effects of Film Holes Position on Anti-icing Characteristics of Aero-engine Inlet Adjustable Blade

Xinwei Jiang(✉), Huan Gong, Yundan Li, Qi Jia, and Miao Li

AECC Shenyang Engine Research Institute, Shenyang, China
690509242@qq.com

Abstract. In order to obtain the influence of film hole position on the anti-icing characteristics of aero-engine inlet adjustable blade, numerical simulation and experimental investigation was carried out for different film hole structure of the blade. The performance of different film hole position (include the trailing edge, the side wall and the rotating shaft of strut) and blowing ratio on the heating effects of the adjustable blade surface were analyzed, and experimental verification was carried out under ice wind tunnel conditions. The results show that with the increasing of blowing ratio, the temperature of adjustable blade increases gradually. The surface with film holes located at the trailing edge has the highest temperature, which is 315 K. Under the same working conditions of mainstream and hot air, the trailing edge inclined hole structure has the smallest ice thickness among the 3 structures. Based on the calculation and experimental results for anti-icing of different positions film hole structures on the adjustable blade, the inclined film holes at the trailing edge has better heating and icing protection effect.

Keywords: film heating · blowing ratio · anti-icing

1 Introduction

The inlet guide vane (IGV) is located at the entrance of aero-engine. Ice can accumulate on the surface of adjustable blade and affect flight safety when the engine operates under icing conditions. Nowadays, Hot Air Anti-Icing System has been widely applied to protect engine inlet components from icing. Numerical simulations and experimental studies have been widely carried out to obtain the icing mechanism [1–4]. The water droplets impingement characteristics of IGV was investigated [5–8], and the distribution of the anti-icing thermal load on the surface was obtained [9].Numerical simulation results show that the inner side of the adjustable part is also a key area requiring anti-icing [10]. It can be seen that previous studies on the icing prevention of engine IGV mainly focused on the water droplet impingement and icing characteristics of the fixed strut part, while relatively few studies have been conducted on the adjustable blade part. Usually, there are film holes on the strut to provide protection to the adjustable blade by blowing and heating.

Chinese Society of Aeronautics and Astronautics (Ed.): CASTC 2023, LNME, pp. 293–299, 2024.
https://doi.org/10.1007/978-981-99-8861-7_30

Based on the above research background, this paper has carried out numerical simulation research on the film heating of adjustable blades, established different film structure calculation models, and focused on the influence of the film hole position on the heating temperature of the adjustable blade surface. And experimental verification under ice wind tunnel conditions has been conducted. The research results will be helpful to design the film anti-icing structure of the adjustable blade and improve the anti-icing ability of aero-engine.

2 Numerical Simulation Methods

In order to study the effects of film hole location on the ice formation of adjustable blades, models with different film holes location were established in the case of adjustable blades having a deflection angle of 30°. The structures are shown in Fig. 1. The film holes are located on the side wall, the trailing edge and rotating shaft of the strut respectively. The hot air film holes are all cylindrical, with a diameter of D = 1mm and a spacing of 2 times the diameter.

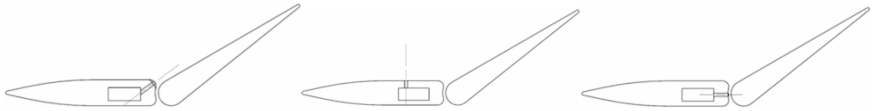

(a)Film holes at trailing edge (b)Film holes at side wall (c)Film holes at the rotating shaft

Fig. 1. Film hole Structures at different positions

The commercial software CFX was used for calculation. The turbulence model was Shear Stress Transport (SST) model, main equations are as follows:

$$\frac{\partial}{\partial t}(\rho k) + \frac{\partial}{\partial x_i}(\rho k u_i) = \frac{\partial}{\partial x_j}\left(\Gamma_k \frac{\partial k}{\partial x_j}\right) + G_k - Y_k + S_k \tag{1}$$

$$\frac{\partial}{\partial t}(\rho \omega) + \frac{\partial}{\partial x_i}(\rho \omega u_i) = \frac{\partial}{\partial x_j}\left(\Gamma_k \frac{\partial \omega}{\partial x_j}\right) + G_\omega - Y_\omega + S_\omega \tag{2}$$

where G_k represents the kinetic energy of turbulence, $G\omega$ express ω equation, $\Gamma\omega$, $\Gamma\omega$ represents the effective diffusion term, Y_k, $Y\omega$ represents the divergence term, $D\omega$ represents the orthogonal divergence term, S_k and $S\omega$ is customized for users.

The blowing ratio (M) is defined as follows:

$$M = \frac{\rho_h u_h}{\rho_g u_g} \tag{3}$$

ρ_h and u_h are the density and velocity of the hot air flow, ρ_g and u_g are the density and velocity of the mainstream.

Given the velocity boundary of the fluid domain inlet, which is 45m/s, and the inlet temperature is 263K.Given the pressure at the outlet, which is calculated based on the

actual aerodynamic parameters of the engine. The blowing ratio (M) of the secondary flow hot air is range of 1.0 to 2.0.

The overall and local grids used for the calculation are shown in Fig. 2. Figure 3 shows the trend of pressure distribution on the surface of adjustable blades with different grid numbers. When the grid size reaches 1.5 million or more, the pressure variation difference on the wall surface of adjustable blades is very small, and the y + is lower than 3.5. Therefore, in the calculation, the mesh size is selected in the numbers of 1.5 to 2 million.

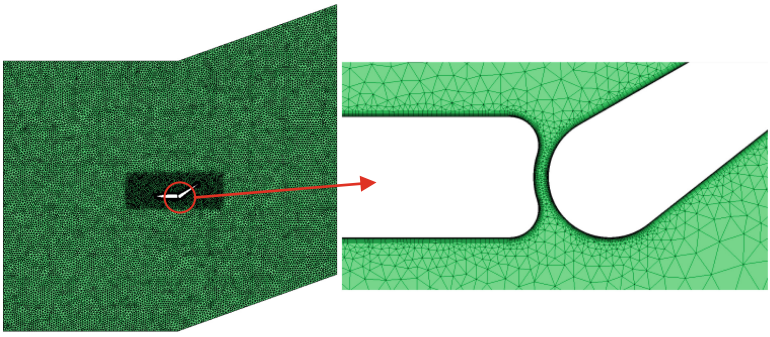

Fig. 2. Grid division of computing domain

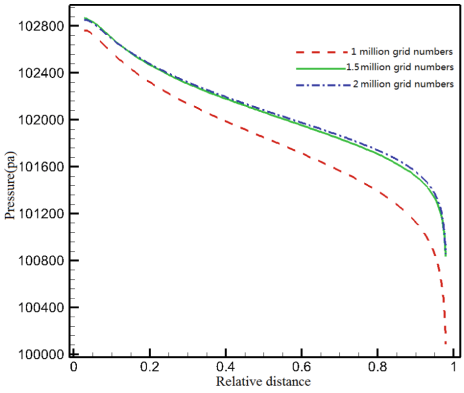

Fig. 3. Comparison of wall pressure with different numbers of grids

3 Numerical Results of Heating Effects

As shown in Figs. 4 and 5, the heating effect comparison of the film in trailing edge under different blowing ratios is shown. According to the cloud images, the wall temperature at the front of the adjustable blade surface is relatively high, while the wall temperature

at the trailing edge is relatively low. An obvious high temperature region is formed on the adjustable blade surface area directly opposite the air film holes. The surface temperature of the adjustable blade gradually decreases along the flow direction. With the increase of blowing ratio, the average surface temperature of the adjustable blade gradually increases. The surface wall temperature of the adjustable blade increases by an average of about 20 k when the blowing ratio increases from 1.0 to 2.0.

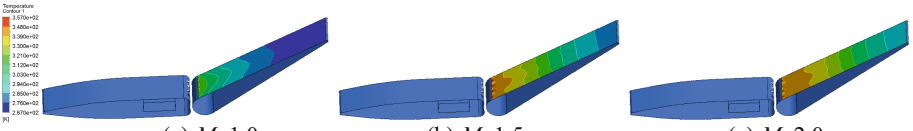

(a) M=1.0 (b) M=1.5 (c) M=2.0

Fig. 4. Wall temperature of the inclined holes structures at the trailing edge of strut

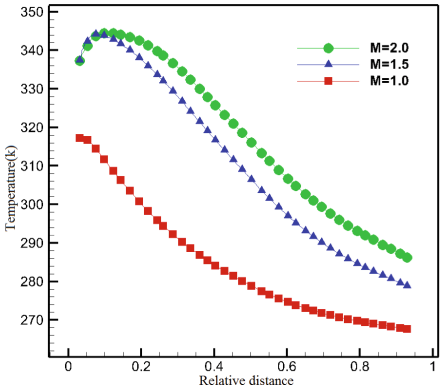

Fig. 5. Wall temperature curves of the inclined holes structure at the trailing edge

Figure 6 shows a comparison curve of the surface wall temperature of adjustable blades with different film hole structures. The trailing edge inclined film hole structure has the best heating effect on adjustable blades, with an average surface temperature of about 315 k. The rotating shaft film hole structure has the worst heating effect, with an average wall temperature of about 269 k.

In order to reveal the influence of different air film structures on the heating characteristics of adjustable blades further, the flow characteristics of different structures are compared and analyzed, as shown in Fig. 7. For the trailing edge inclined hole structure, all secondary flow hot air can better attach to the blade surface, and has a higher outflow speed, while less diffusion to the mainstream, forming a better protective effect on the blade concave surface. For the side wall film hole structure, due to the influence of the position and direction of the film outflow, its normal momentum is relatively larger, resulting in more mixing into the mainstream. At the same time, due to the reduced momentum after reaching the adjustable blade, a part of the hot gas is pumped to the convex surface of the blade, resulting in a reduced protective effect on the adjustable

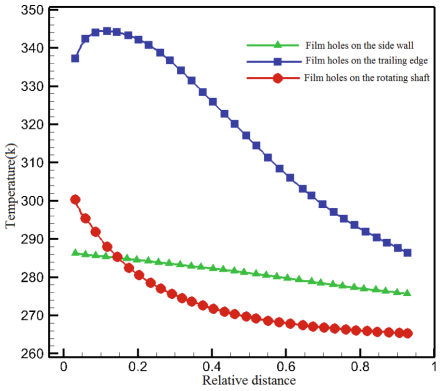

Fig. 6. Comparison of heating effect of different film hole structure

blade. For the rotating shaft film hole structure, due to its relatively close distance to the blade convex side, most of the hot air is pumped to the convex surface due to the suction effect, and only a small portion attach to the surface of the blade concave side, resulting in a waste of hot air so its heating effect is the worst .

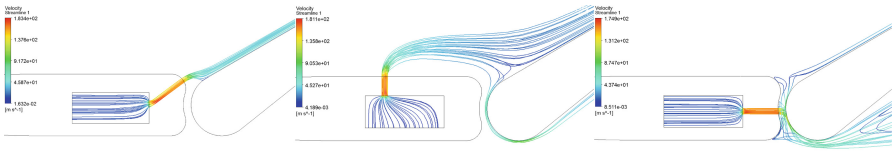

(a)Film holes on trailing edge (b)Film holes on side wall (c)Film holes on the rotating shaft

Fig. 7. Comparison of streamline of different film hole structure

4 Experimental Results of Ice Wind Tunnel

In order to further verify the anti-icing effect of different position air film structures on adjustable blades, preliminary anti-icing effect tests on different structure test pieces were conducted in an ice wind tunnel. The structure of the experimental system is shown in Fig. 8.

The facility is composed of eleven parts, including wind tunnel, air dynamic system, cooling system, atomization water spray system, vacuum system, secondary flow system, circulating water system, softening water system, corner heat system, controlling system, viewing system and corresponding auxiliary systems. The icing wind tunnel is located in AECC Shenyang Engine Research Institute, which is mainly used for engine inlet cones, struts and other inlet components tests and verifications.

Figure 9 shows the photos of the experimental results for different structures under the same icing conditions. It can be seen that adjustable blades with different structures all accumulate with a certain thickness ice. However, the amount of ice on the surface

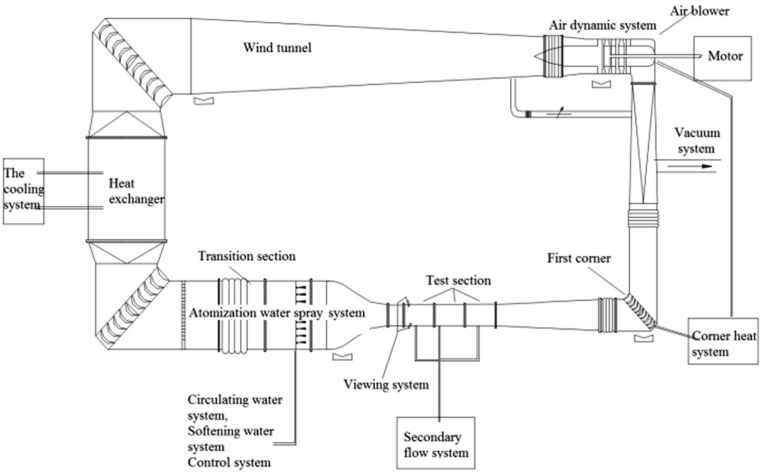

Fig. 8. Experimental systems

of different structure is different. The side wall film hole structure shows significant ice accumulation, with a maximum ice thickness of about 5 mm. The trailing edge inclined hole structure has the smallest ice thickness, and there are obvious marks of film impact on the surface of the blade. The ice amount directly facing the film hole is very small, with a maximum ice thickness about 3mm. Finally, for blade with film hole structure on the rotating shaft, severe icing occurred on the adjustable blade surface, with a maximum icing thickness of about 8 mm.

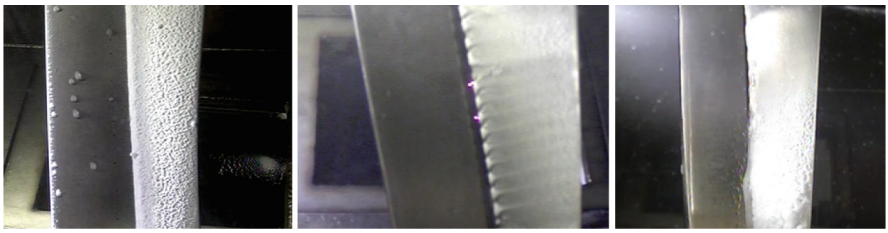

(a)Film holes at the side wall (b)Films hole at the trailing edge (c)Film holes at the rotating shaft

Fig. 9. Icing test results of different film hole structures

Comparing the ant-icing experimental results of adjustable blades with three structures, the trailing edge inclined hole structure has the best protective effect on adjustable blades, which is also consistent with the calculated conclusions of heating effects. It is recommended to consider both the location of the hot air film hole and the realizable film structure during engineering design. When the hot air temperature and flow rates are constant, refer to the performance of the film hole position in this paper to achieve effective icing protection for adjustable blades.

5 Conclusions

In this study, numerical simulations and experiments were carried out to acquire the anti-icing performances of inlet adjustable blade with different film hole structures. The following conclusions can be obtained.

(1) As the blowing ratio increases, the heating effect of different film structures on adjustable blades increases. When the blowing ratio is increased from 1.0 to 2.0, the maximum wall temperature of adjustable blades with different structures increase by about 20 K.
(2) The trailing edge inclined hole structure has a good heating effect, with a maximum average wall temperature of about 315 K.
(3) A portion of the hot air coming out of the film holes will be sucked to the convex surface of the blade. The lower the blowing ratio, the more obvious the suction effect is. When the blowing ratio is 2.0, the trailing edge inclined hole structure hot air can fully attach to the blade surface.
(4) According to the ice wind tunnel verification results, the trailing edge inclined hole structure has the best icing protection ability to adjustable blades, consistent with the calculated conclusions.

References

1. Sang, L., Eric, L.: Simulation of icing on a cascade of stator blades. J. Propulsion Power **24**(6) (2008)
2. Papadakis, M., Yeong, H.W., Wong, S.C., et al.: Comparison of experimental and computational ice shapes for an engine inlet. In: AIAA Atmospheric and Space Environments Conference, Toronto (2010)
3. Pellissier, M., Habashi, W., Pueyo, A.: Design optimization of hot-air anti-Icing systems by FENSAP-ICE. In: 48th AIAA Aerospace Sciences Meeting Including the New Horizons Forum and Aerospace Exposition, Orlando, Florida (2010)
4. Guido, S., Baruzzi, M.O., et al.: Multi-physics simulation of aircraft ice protection system and ice impact with turbofan blades. In: 8th AIAA Atmospheric and Space Environments Conference, Washington, D.C (2016)
5. Yang, J., Guo, W., Lou, D.: Numerical analysis of trajectories of water droplets on the anti-icing vane of an engine. Gas Turbine Exper. Res. **24**(1), 19–24 (2011)
6. Liu, H., Yang, J.: Effect of film gap outflow on water droplets impingement characteristics of the anti-icing vane. Gas Turbine Exper. Res. **30**(2), 51–57 (2017)
7. Ke, P., Zhang, Y., Yu, G., et al.: Influence of exterior hot-film on droplet impingement characteristics over aero-engine inlet strut. J. Aerospace Power **32**(3), 621–629 (2017)
8. Zhao, J., Wu, D.: Effects of regulated angles to droplet impingement characteristics of aero-engine strut. Aeronau. Comput. Tech. **43**(4), 61–64 (2013)
9. Xu, L., Zhou, J., Zhang, D., et al.: Numerical simulation of anti-icing heat load for strut of aero-engine inlet. Aeroengine **35**(4), 21–24 (2009)
10. Yaguo, L., Zhenxia, L., Lifen, Z., et al.: Numerical simulation of ice accretions on trailing adjusted strut. Aeronau. Comput. Tech. **41**(6), 58–65 (2011)